

## Low-Energy Neutral Pion Photoproduction in $H_2$ and He

A. ODIAN,\* G. STOPPINI,† AND T. YAMAGATA‡  
*University of Illinois, Urbana, Illinois*

(Received July 11, 1960)

The results of an experiment on the photoproduction of neutral pions from  $H_2$  and He in the very low-energy region are compared with the dispersion relation calculations of Chew, Goldberger, Low, and Nambu (C.G.L.N.). For  $H_2$ , agreement was found for incident  $\gamma$ -ray energies above 155 Mev for  $N^{(+)} \approx +0.065$  and disagreement below for all constant values of  $N^{+}$ . The He results give support to the C.G.L.N. effective-range formulas for the small  $p$ -wave phase shifts.

### INTRODUCTION

THE Chew-Goldberger-Low-Nambu (C.G.L.N.) dispersion relation calculations on photoproduction of pions have generally been in agreement with experiment.<sup>1</sup> The presence of the large ( $\frac{3}{2}, \frac{3}{2}$ ) and direct interaction terms, however, have made it rather difficult to check the smaller terms which appear in the  $\mathcal{F}^{(0)}$  amplitude. An experiment which has had some bearing on those terms, is the angular and energy dependence of the  $\pi^-/\pi^+$  ratio from deuterium. These depend quite critically on the  $\mathcal{F}^{(0)}$  amplitude. There is some ambiguity in the comparison, but the agreement is not very good.<sup>2</sup> These small terms could also possibly be the source of the deviations which seem to exist in the comparison with the experimental c.m.  $90^\circ$  differential cross sections of positive pion photoproduction,<sup>3</sup> even when the real electric dipole term  $N^{(-)}$  is properly evaluated.<sup>4</sup>

In this paper the C.G.L.N. formulas are used as they stand. Now it seems more and more evident that these formulas should be modified to take into account the high-energy contribution within the dispersive integrals by using subtracted dispersion relations. Also the C.G.L.N. formulas do not contain the effect of the pion-pion interaction which could be important and might affect the  $\mathcal{F}^{(0)}$  amplitude at all energies. Obviously, the addition of the mentioned terms does not change the main features of the C.G.L.N. predictions, but would only improve the detailed understanding of photomesonic processes. A possible experimental determination of these terms could give some important theoretical indications.

The experiments discussed in this paper have been analyzed with the aim of getting some information on the  $S$ -wave term in the amplitude for the photoproduction of neutral pions in hydrogen. In the C.G.L.N. framework, such a term at low energies gives one of the

largest contributions to the  $\mathcal{F}^{(0)}$  amplitude. The experiments consisted in measuring excitation curves for the processes

$$\gamma + p \rightarrow \pi^0 + p, \quad (1)$$

$$\gamma + \text{He} \rightarrow \pi^0 + \text{He}, \quad (2)$$

by a  $\gamma$ - $\gamma$  coincidence method, and using the threshold determination of the process

$$\gamma + p \rightarrow \pi^+ + n, \quad (3)$$

as an x-ray beam energy calibration. The comparison between processes (1) and (2) presents some interesting features, mainly because of the absence in process (2) of any contribution from  $S$ -wave pion production. In fact such a transition is always associated with a spin flip of the parent nucleon. Such a spin flip would break the original He nucleus leading to an inelastic process. When the incident x-ray energy is less than 160 Mev, all neutral pions produced from He must be elastically produced as there is not enough energy to both break up the  $\alpha$  particle and produce a neutral pion. The data below reported refer to an x-ray energy interval from threshold to 170 Mev.

In this same energy region, the angular distribution of  $\pi^0$ 's from  $H_2$  deduced by the C.G.L.N. theoretical formulas is quite sensitive to the unknown real electrical dipole term  $N^{(+)}$  and also depends on the choice of the small  $p$ -wave scattering phase shifts. This could be a serious difficulty because the actual experimental knowledge of the small  $p$ -wave scattering phase shifts is quite confused and, in practice, one then has several more adjustable parameters besides the pion nucleon coupling constant. Fortunately in the energy region of this experiment, the largest terms for process (1) contain the small  $p$ -wave phase shifts in the same combination as that which appears in the terms for process (2), in which  $N^{(+)}$  does not appear. So, if the  $\alpha_{33}$  phase shift is experimentally known for c.m. pion momenta  $0 \leq q \leq 0.55$ , it is possible to derive from process (2) information on the small  $p$ -wave phase shifts, reducing the unknowns for the discussion of process (1). The term  $N^{(+)}$  whose evaluation seems to be quite troublesome still remains unknown. The absolute value and energy dependence of this term will be discussed on the basis of the experimental results below reported.

\* Now Fulbright Fellow at the Istituto Superiore di Sanità, Rome, Italy.

† Now at the Istituto di Fisica dell'Università, Rome, Italy.

‡ Now Ford Foundation Fellow at CERN, Geneva, Switzerland.

<sup>1</sup> G. F. Chew, M. L. Goldberger, F. E. Low, and Y. Nambu, Phys. Rev. **106**, 1345 (1957); W. S. McDonald, V. Z. Peterson, and D. R. Corson, Phys. Rev. **107**, 577 (1957).

<sup>2</sup> M. Beneventano, G. Bernardini, G. Stoppini, and L. Tau, Nuovo cimento **10**, 1109 (1958).

<sup>3</sup> M. Beneventano, G. Bernardini, D. Carlson-Lee, G. Stoppini, and L. Tau, Nuovo cimento **4**, 323 (1956).

<sup>4</sup> H. Munczek and M. Cini (private communication).

A further result of the experiment is a measurement of the neutral pion mass produced in processes (1) and (2). In both cases the result is in agreement with the measurements done by using the zero kinetic energy charge exchange scattering of negative pions on protons. This adds some evidence against the existence of Baldin's  $\pi_0^0$  meson.<sup>5</sup>

Luckey *et al.*<sup>6</sup> have recently published the angular distribution for process (1) at  $\gamma$ -ray energies of 170 Mev and 190 Mev. The comparison with the C.G.L.N. formulas shows good agreement if  $N^{(+)}=0.04$  is assumed. Another measurement of the angular distribution for  $E_\gamma=160$  Mev and above has been published by Vasilkov *et al.*<sup>7</sup> An angular distribution as a function of the energy is contained in a thesis by Modesitt.<sup>8</sup>

The total cross section for process (1) for energies larger than 150 Mev is given by Koester and Mills<sup>9</sup> and also by Vasilkov *et al.*<sup>10</sup>

### 1. EXPERIMENTAL APPARATUS AND RESULTS

The experiments have been performed using the x-ray beam of the 300-Mev betatron of the University of Illinois. The appendix or liquid hydrogen container used was cylindrical in shape, and coaxial with the beam. The length of the cylinder was 11.4 cm and its diameter was 10.2 cm. The beam diameter at the position of the target was 5 cm. The entrance and exit windows were made of 5 mil thick Mylar to reduce background. The walls of the cylinder were made of 3 mil copper.

#### $\pi^0$ Experiments

The counters for the  $\pi^0$  experiments from hydrogen and helium, consisted of two total absorption lead glass Čerenkov counters which were used in coincidence to

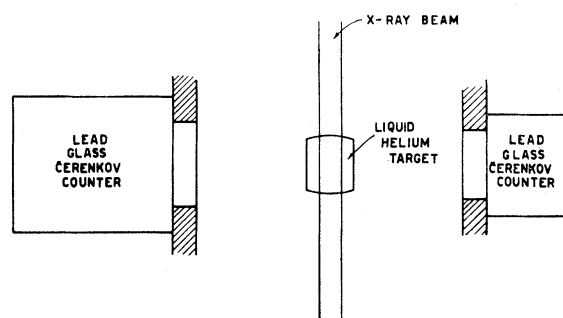


FIG. 1.  $\pi^0$  experiment layout.

detect the two  $\gamma$  rays from the decay of the  $\pi^0$  meson. As shown in Fig. 1 each of these Čerenkov counters was placed at  $90^\circ$  to the x-ray beam and were  $180^\circ$  apart. This arrangement has a definite advantage as a threshold detector since the probability of the two decay photons going into the two Čerenkov counters is the largest for a  $\pi^0$  at rest, and decreases rapidly at higher energies. The cylindrical lead glass blocks had diameters of 12 radiation lengths and thicknesses of 15 radiation lengths. Heavy lead collimators were placed in the front of the lead glass to reduce the entrance diameter to prevent the escape of the shower. Before the experiment, the counters were calibrated using monoenergetic electrons of energies from 70 to 120 Mev, produced in a lead target and magnetically analyzed. The full width at half maximum of the pulse-height distributions in the Čerenkov counters was about 60% at the lowest energy, and the positions of the peaks of the distributions were linear with the energy. The distance of the front of the Čerenkov counters from the center of the appendix was 14 in. The lead glass was viewed from the rear by twelve 6342 RCA phototubes. The summed outputs in each of these counters were amplified, limited, and put into coincidence with a resolving time  $2\tau$  of  $1.4 \times 10^{-8}$  sec. Before being limited, these pulses were split, with one part going to the limiter and the other part to a discriminator and then to a scaler. In this way the singles counting rate was monitored in each of the counters to insure against drift. Every hour during the cooling break of the betatron, a pulser was connected at the position of the Čerenkov counters and the pulse heights at the input of the limiters checked to guard against drifts in the gains of the distributed amplifiers. Every several days a pulsed light source was attached to the front of each of the Čerenkov counters to equalize the outputs of the phototubes and standardize them. The gains of the amplifiers were such that pulses corresponding to 25 Mev photons were limited to insure against losses in the counting rate due to the Doppler shifting in the  $\gamma$ -ray energy from the  $\pi^0$  decay toward lower energies.

The coincidence counting rate was observed as a function of the maximum energy of the bremsstrahlung for energies below the threshold to 170 Mev. The maximum energy of the betatron was moved in steps of 2.5 Mev up to 160 Mev, and then in 5 Mev steps to 170 Mev. The resulting curve of the counting rate vs the maximum energy of the betatron is called a yield curve. Runs were taken with the appendix empty and also by delaying one of the inputs by 32 nanoseconds to determine the accidental rate at all energies of the betatron. The singles counting rates were only slightly dependent on the energy setting of the betatron and hence the accidental rate was also about independent of the energy. The accidental rate and the empty target rate were equal within statistics. The subtraction of the background was performed by taking as background the average rate of the accidentals at the various betatron

<sup>5</sup> A. M. Baldin and P. K. Kabir, *Nuovo cimento* **9**, 547 (1958).

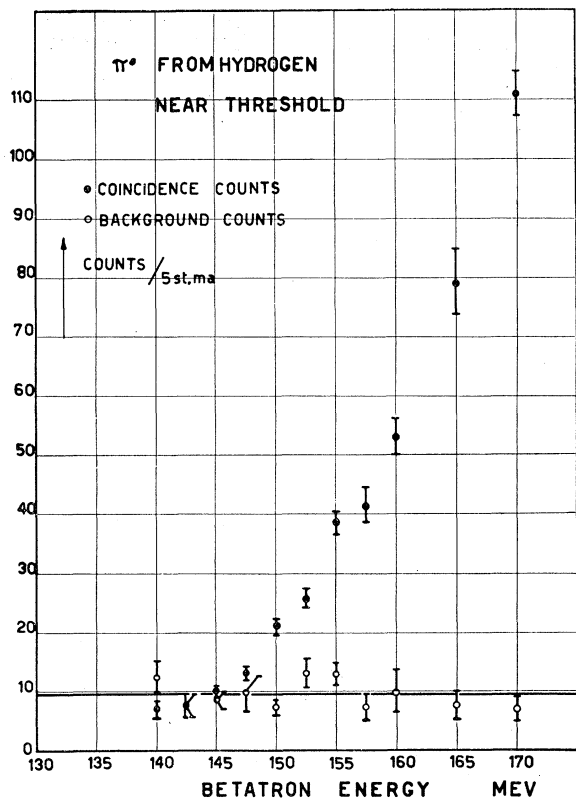
<sup>6</sup> P. D. Luckey, L. S. Osborne, and J. J. Russell, *Phys. Rev. Letters* **3**, 240 (1959).

<sup>7</sup> R. G. Vasilkov, B. B. Govorkov, and V. I. Goldauskii, *J. Exptl. Theoret. Phys. (U.S.S.R.)* **37**, 317 (1959) [translation: *Soviet Phys. JETP* **37**, 224 (1960)].

<sup>8</sup> G. E. Modesitt, thesis, University of Illinois, 1958 (unpublished).

<sup>9</sup> L. J. Koester and F. E. Miles, *Phys. Rev.* **105**, 1900 (1957).

<sup>10</sup> R. G. Vasilkov and B. B. Govorkov, *J. Exptl. Theoret. Phys. (U.S.S.R.)* **37**, 11 (1959) [translation: *Soviet Phys. JETP* **37**, 7 (1960)].

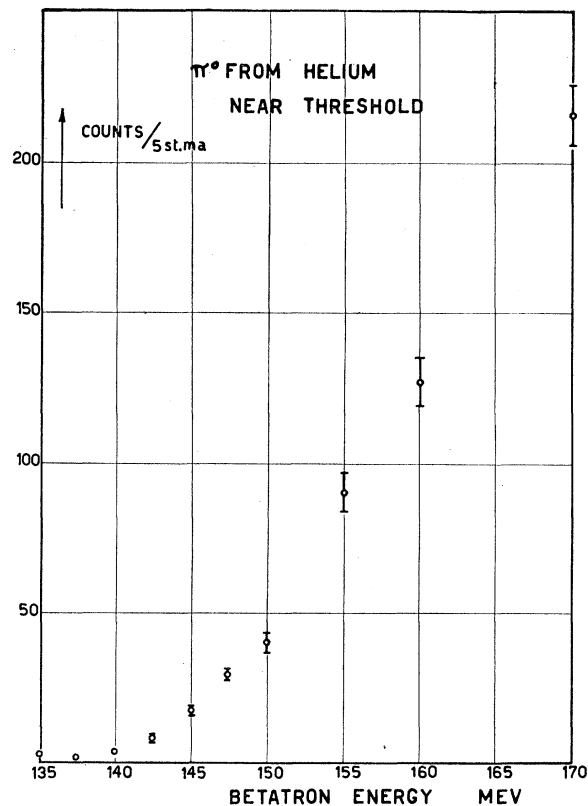
FIG. 2. Experimental yield from the process  $\gamma + p \rightarrow \pi^0 + p$ .

energies. The real counting rate was very small when the x-ray maximum energy was very close to threshold, so that in order to prevent pickup from simulating good events, both of the pulses which formed the coincidence were also displayed on a 517 A Tektronix oscilloscope and photographed.

The efficiency for the detection of  $\gamma$ - $\gamma$  coincidences in the sketched experimental situation depends on the kinetic energy and laboratory angle of emission of the  $\pi^0$ . Such efficiency depends also strongly on the extension of the source and of the detectors. The yield of double coincidences at each betatron energy is proportional to the integral of the cross section from threshold to  $E_{\max}$  properly weighted by the bremsstrahlung spectrum and the detection efficiency function. In Fig. 2 is shown the graph of the experimental yields as a function of the maximum x-ray energy for process (1). In Fig. 3 is shown the experimental yield curve obtained with the appendix filled with liquid He.

#### $\pi^+$ Experiment

The same target was used in the  $\pi^+$  from  $H_2$  experiment as in the  $\pi^0$  experiments. The counters were changed, however, to detect the decay positron of the  $\mu^+$  meson resulting from the decay of the  $\pi^+$  meson. At low x-ray energies where the data have been collected, most of the  $\pi^+$ 's created also stop in the large liquid

FIG. 3. Experimental yield from the process  $\gamma + He^4 \rightarrow \pi^0 + He^4$ .

hydrogen target. The  $\mu^+$ 's also remain within the target. Thus, by counting electrons in the backward direction to the x-ray beam, the total cross section for  $\pi^+$  photo-production can be measured with very little contribution from electron positron pair production. In any case, this background can be subtracted out by running at energies below the threshold. The method is the same as the one used by Penner *et al.*<sup>11</sup> in a similar experiment.

The decay positron counter consisted of a two counter telescope whose counters are called *A* and *B* (Fig. 4). Counter *B* was a Čerenkov counter which consisted of a Lucite cylinder 12.5-cm diameter and 12.5 cm long, viewed by a single 5 in. photomultiplier RCA 7046. Two different counters *A* and *A'* were used in different runs. One was a liquid scintillator cell 7.5 cm in diameter and 5 cm thick. The other was a 5 cm thick block of Lucite viewed on the edge by a single RCA 6810A phototube. In two runs, the coincidence rate between *A* and *B* were counted as a function of the maximum betatron energy. The singles rate of *B* was found to be a strong function of the x-ray maximum energy so that these data were also taken into consideration. All the data were collected with the telescope set at an angle of  $100^\circ$  with respect to the x-ray beam. In Fig. 5 is shown a typical curve of the counting rate per  $\frac{1}{2}$  standard monitors as a function of the nominal maximum energy

<sup>11</sup> S. Penner, thesis, University of Illinois, 1956 (unpublished).

of the x-ray beam. The efficiency for counting events will in general be a function of the angles and energies of the outgoing products. Thus, the yield is an integral over the x-ray energies of the differential cross section for process (3), properly weighted with an efficiency function and with the bremsstrahlung spectrum. In the  $\pi^+$  case, the efficiency function was not determined in absolute value. Actually an absolute calculation of the efficiency function would imply an evaluation of the positron scattering and annihilation in the telescope, and also of the effective energy bias of the telescope. The geometry and the bias were chosen to diminish the background and to increase the counting rate, and not to guarantee the smallness of effects such as scattering or allow a reliable evaluation of them. The interest of this measurement was not in studying process (3) but to use it to get an absolute energy calibration of the betatron. To this end, it is only necessary to know the dependence of the efficiency function on the x-ray energy and to be sure that the recorded events were ascribable to positrons. This second circumstance is guaranteed by the use of Čerenkov counters at a large angle.

As is obvious for an experiment of the kind outlined above, the betatron energy stability is very essential. This point has been checked by several high counting rate experiments which have shown that the rms stability and reproducibility of the betatron energy is better than 0.25 Mev.<sup>11</sup>

## 2. $\pi^0$ DETECTION EFFICIENCY CALCULATION

Consider an  $\pi^0$  with velocity  $c\beta$  going in the direction  $\theta, \varphi$  with respect to the x-ray beam. Take an area

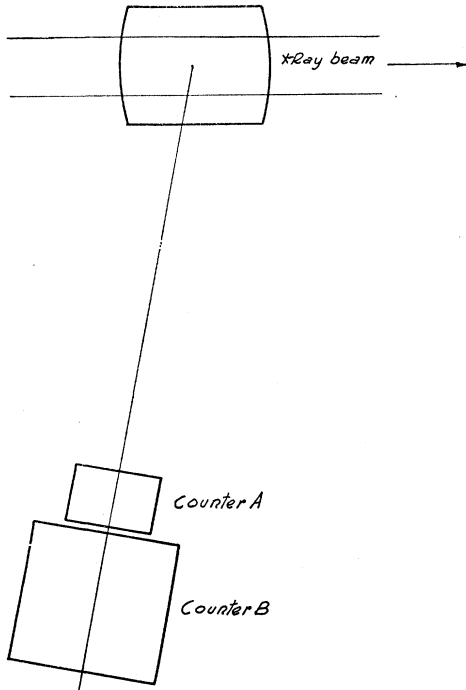


FIG. 4.  $\pi^+$  experiment layout.

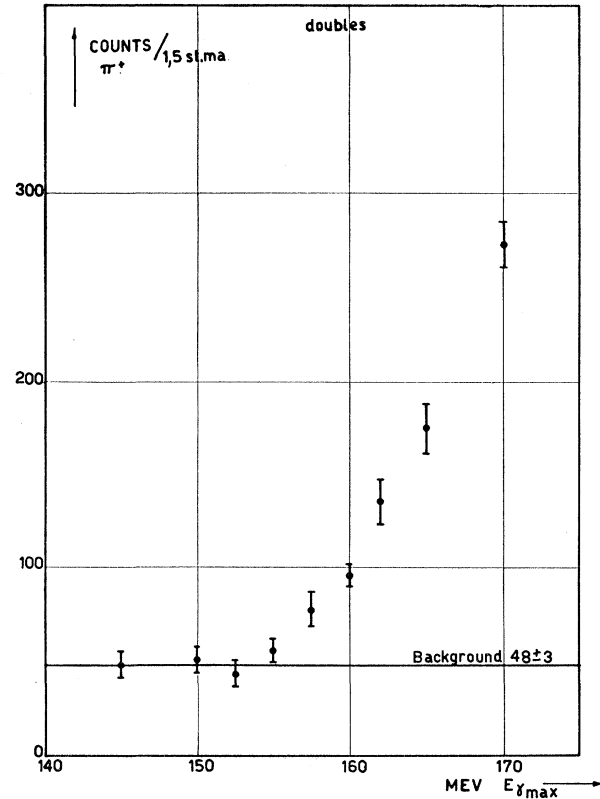


FIG. 5. Experimental yield from the process  $\gamma + p \rightarrow \pi^+ + n$ .

element  $dA_1$  in the aperture of the first Čerenkov counter, and let the solid angle subtended by that area at the point of the decay be  $d\Omega_1$ . Then, the probability that one of the decay photons goes into this solid angle is given by  $(1/2\pi)(d\Omega_1^*/d\Omega_1)d\Omega_1$ , where  $d\Omega_1^*$  is the solid angle transformed into the rest frame of the  $\pi^0$ . The direction of the other decay photon is uniquely determined. Define a function  $\epsilon$  which takes the value 1 when the other photon enters the aperture of the second Čerenkov counter and 0 if it does not. Then the efficiency of detection of a  $\pi^0$  by the two-counter geometry is given by

$$f(\theta, \varphi, \beta) = \frac{1}{2\pi} \int_{A_1} \epsilon \frac{d\Omega_1^*}{d\Omega_1} d\Omega_1,$$

where  $d\Omega_1$  is integrated over  $A_1$ , the aperture of the first Čerenkov counter.

In the case of a point target with two Čerenkov counters 180° apart, the detection efficiency is symmetric about the axis of the counters. So, it may be written as  $f(\beta, \alpha)$ , where  $\alpha$  is the angle between the axis and the direction of  $\pi^0$ . Figure 6 shows the result obtained by a calculation using "Illiac." As is expected, the detection efficiency is uniform at zero energy. At higher energies only those  $\pi^0$ 's which go in the direction of either of two counters are detected. The 0°–180°

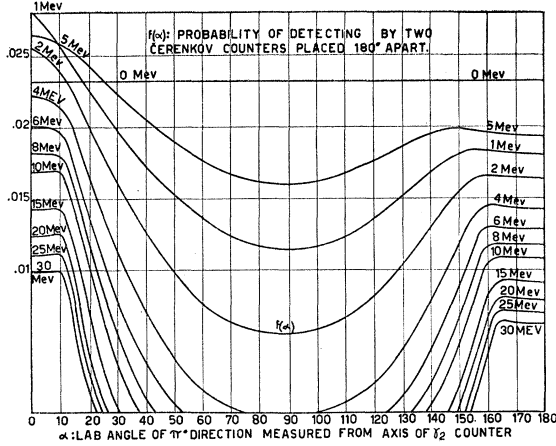


FIG. 6. Probability of detecting a  $\pi^0$  of kinetic energy from 0 to 30 Mev by two Čerenkov counters placed  $180^\circ$  apart. The probability is given as a function of the angle between the  $\pi^0$  direction and the axis of the two counters.

asymmetry comes from difference in size of two Čerenkov counters employed. The actual target had non-negligible size and therefore was divided into 100 subvolumes. The efficiency was calculated for each subvolume and averaged.

From the curves of Fig. 6 another family  $F(T_{\pi^0}, \theta_{\pi^0})$  was derived by changing  $\alpha$  to  $\theta_{\pi^0}$ . To make this transformation, an integration was performed over the  $\varphi$  direction. This second family is shown in Fig. 7 in solid lines. The dashed lines are the result of assuming a point source for the  $\pi^0$ 's. The disagreement shows that this is a bad assumption.

Up to this point the results are applicable to both  $\pi^0$ 's from  $H_2$  and He. Next a transformation was made from the variables  $T_{\pi^0}$  and  $\theta_{\pi^0}$  to  $E_\gamma$  and  $\theta^*_{\pi^0}$ , the incident x-ray energy and the center-of-mass pion angle. To make this transformation, the kinematics of the reaction were used and hence two sets of functions  $F(E_\gamma, \theta^*_{\pi^0})$  were obtained, for  $H_2$  and He.

Then the theoretical yield curve is given by

$$Y(E_\gamma) = K(E_\gamma) \int_{E_{\gamma th}}^{E_\gamma} dE'_\gamma \varphi(E'_\gamma) \int_0^\pi d\theta^*_{\pi^0} \times \frac{d\sigma}{d\Omega^*}(E'_\gamma, \theta^*_{\pi^0}) F(E'_\gamma, \theta^*_{\pi^0}) \sin\theta^*_{\pi^0},$$

where  $\varphi(E'_\gamma)dE'_\gamma$  is the bremsstrahlung spectrum corresponding to a maximum energy  $E_\gamma$ , and  $K(E_\gamma)$  depends on the number of atoms in the beam and on the energy contained in one monitor unit for a maximum energy  $E_\gamma$ . For  $\pi^0$ 's from  $H_2$ , the differential cross section can be written as

$$d\sigma/d\Omega^* = A + B \cos\theta^*_{\pi^0} + C \cos^2\theta^*_{\pi^0},$$

where  $A$ ,  $B$ , and  $C$  are functions of  $E'_\gamma$ . Thus  $Y(E_\gamma)$

becomes

$$Y_{H_2}(E_\gamma) = K_{H_2}(E_\gamma) \left\{ \int_{\gamma th}^{E_\gamma} A F_A \varphi dE'_\gamma + \int_{E_{\gamma th}}^{E_\gamma} B F_B \varphi dE'_\gamma + \int_{E_{\gamma th}}^{E_\gamma} C F_C \varphi dE'_\gamma \right\},$$

where

$$F_A = \int_0^\pi F_{H_2}(E'_\gamma, \theta^*_{\pi^0}) \sin\theta^*_{\pi^0} d\theta^*_{\pi^0},$$

$$F_B = \int_0^\pi F_{H_2}(E'_\gamma, \theta^*_{\pi^0}) \sin\theta^*_{\pi^0} \cos\theta^*_{\pi^0} d\theta^*_{\pi^0},$$

$$F_C = \int_0^\pi F_{H_2}(E'_\gamma, \theta^*_{\pi^0}) \sin\theta^*_{\pi^0} \cos^2\theta^*_{\pi^0} d\theta^*_{\pi^0}.$$

The curves  $F_A$ ,  $F_B$ , and  $F_C$  as a function of energy are shown in Fig. 8.

For elastic  $\pi^0$ 's from He, the differential cross section can be written as

$$d\sigma/d\Omega^* = C \sin^2\theta_{\pi^0} F_r^2(q^2),$$

where  $C$  is a function of energy and  $F_r^2(q^2)$  is the form factor of He.  $F_r^2(q^2)$  is a slow function of angle. This dependence was neglected especially since the efficiency

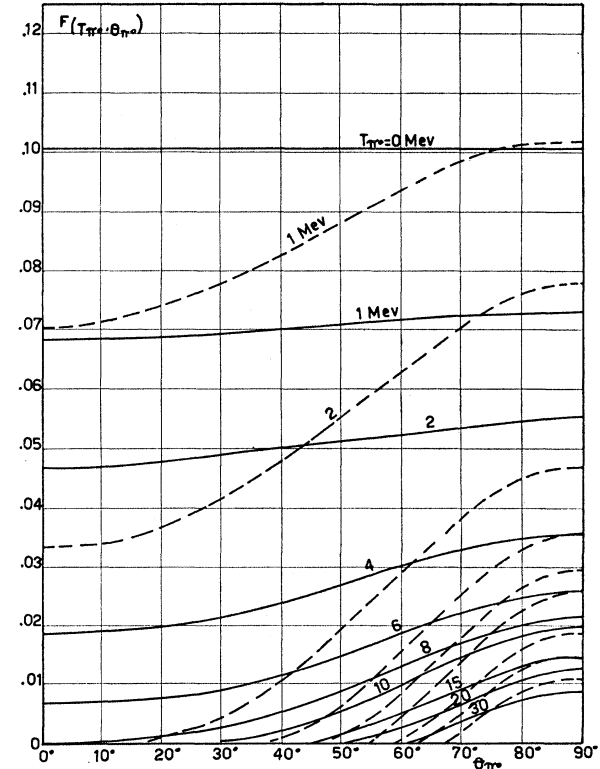


FIG. 7. Probability of detecting  $\pi^0$  of kinetic energy  $T_{\pi^0}$  as a function of the lab emission angle  $\theta_{\pi^0}$  with respect to the  $\gamma$ -ray beam. The dashed lines refer to a point source.

peaked at 90° in the laboratory system. Thus

$$Y_{\text{He}}(E_\gamma) = K_{\text{He}}(E_\gamma)$$

$$\times \int_{E_{\gamma\text{th}}}^{E_\gamma} C(E_\gamma') F_{\text{He}}(E_\gamma') F_{\gamma^2}(E_\gamma') \varphi(E_\gamma') dE_\gamma',$$

where

$$F_{\text{He}}(E_\gamma') = \int_0^\pi F_{\text{He}}(E_\gamma', \theta_{\pi^0}^*) \sin^3 \theta_{\pi^0}^* d\theta_{\pi^0}^*.$$

$F_{\text{He}}$  is shown in Fig. 9.

### 3. $\pi^+$ DETECTION EFFICIENCY CALCULATION

The method used for studying process (3) was to detect the electron decay of the decay chain  $\pi^+ \rightarrow \mu^+ \rightarrow e^+$ . The detected fraction of the pions created by x-rays of fixed energy  $E_\gamma$  depends on the emission laboratory  $\pi^+$  angle  $\theta_{\pi^+}$ . The excitation function for positron detection is

$$Y_+(E_\gamma) = K_{\text{H}_2'}(E_\gamma) \int_0^\pi \int_{E_{\gamma\text{th}}}^{E_\gamma} \frac{d\sigma_+}{d\Omega^*} F_+(E_\gamma', \theta_{\pi^+}^*) \times \varphi(E_\gamma') dE_\gamma' \sin \theta_{\pi^+}^* d\theta_{\pi^+}^*,$$

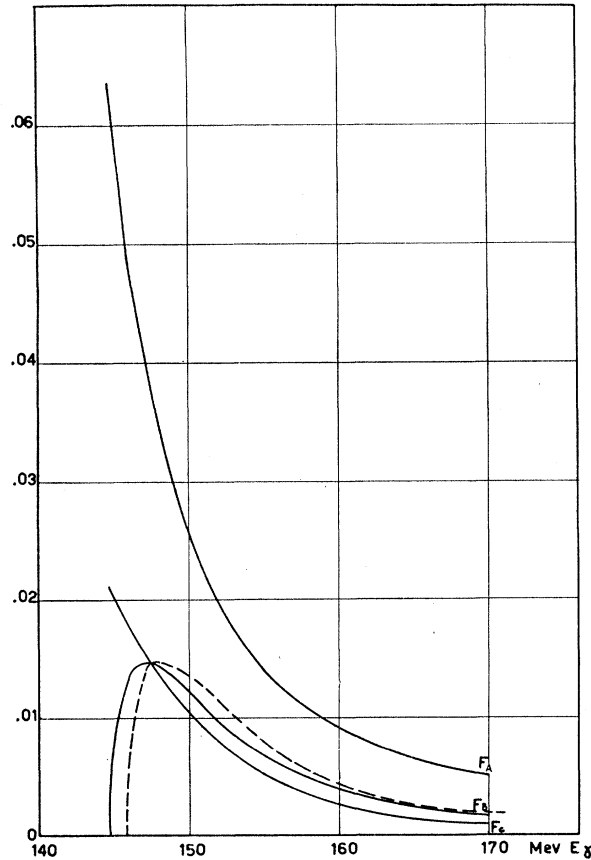


FIG. 8. The efficiency functions  $F_A$ ,  $F_B$ ,  $F_C$  as a function of the  $\gamma$ -ray energy.  $m_0 = 135$  Mev has been assumed. Only for  $F_B$  is shown the curve obtained by assuming  $m_0 = 136$  Mev.

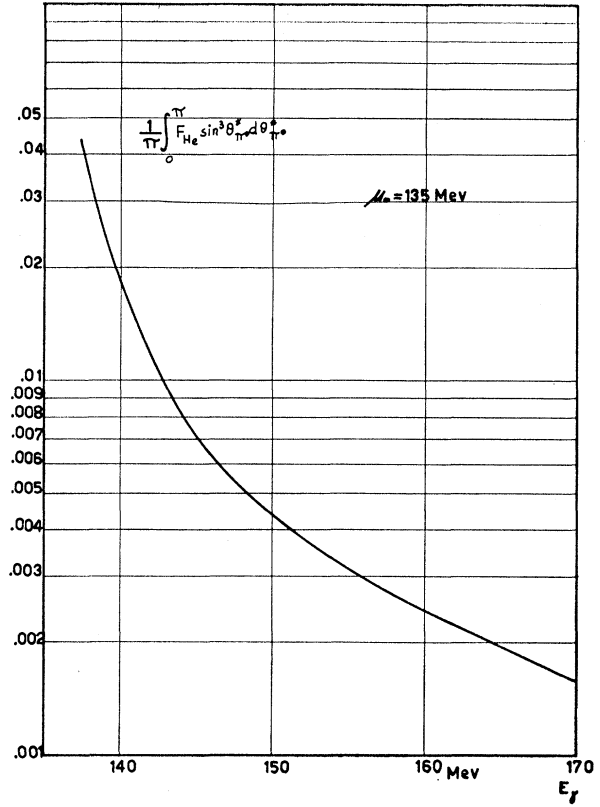


FIG. 9. The function  $F_{\text{He}}$  as a function of  $E_\gamma$ . Line .03 should read  $m_0 = 135$  Mev.

where  $F_+(E_\gamma', \theta_{\pi^+}^*)$  represents the efficiency for the detection of a positron when the  $\pi^+$  is created at a c.m. angle  $\theta_{\pi^+}^*$  by an x-ray of energy  $E_\gamma'$ . From threshold to 170 Mev, the c.m. angular distribution can be represented by

$$d\sigma_+/d\Omega^* = W(a_0 + a_1 \cos \theta_{\pi^+}^* + a_2 \cos^2 \theta_{\pi^+}^*),$$

where  $W$  is the phase space,  $\theta_{\pi^+}^*$  is the c.m. emission angle of the  $\pi^+$  and  $a_0$ ,  $a_1$ , and  $a_2$  are functions of  $E_\gamma'$ . Thus

$$Y_+(E_\gamma) = K_{\text{H}_2'}(E_\gamma) \left[ \int_{E_{\gamma\text{th}}}^{E_\gamma} F_0 a_0 W \varphi dE_\gamma' + \int_{E_{\gamma\text{th}}}^{E_\gamma} F_1 a_1 W \varphi dE_\gamma' + \int_{E_{\gamma\text{th}}}^{E_\gamma} F_2 a_2 W \varphi dE_\gamma' \right],$$

where

$$F_0 = \frac{1}{2\pi} \int_0^\pi F_+(E_\gamma', \theta_{\pi^+}^*) \sin \theta_{\pi^+}^* d\theta_{\pi^+}^*,$$

$$F_1 = \frac{1}{2\pi} \int_0^\pi F_+(E_\gamma', \theta_{\pi^+}^*) \sin \theta_{\pi^+}^* \cos \theta_{\pi^+}^* d\theta_{\pi^+}^*,$$

$$F_2 = \frac{1}{2\pi} \int_0^\pi F_+(E_\gamma', \theta_{\pi^+}^*) \sin \theta_{\pi^+}^* \cos^2 \theta_{\pi^+}^* d\theta_{\pi^+}^*.$$

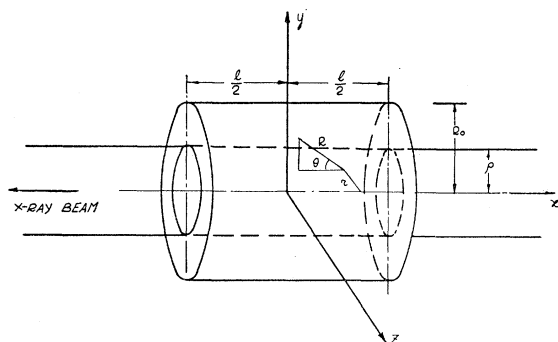


FIG. 10. Target geometry.

If  $\pi^+$ 's are uniformly produced in the region of the intersection of the x-ray beam with the hydrogen target (Fig. 10), a pion of range  $R$  produced from a point a distance  $r$  from the axis of the beam, a distance  $x$  along the axis, and at an angle  $\theta_{\pi^+}$  with respect to the beam, has a probability of staying within the hydrogen target of  $P_{\pi}(r, R, \theta_{\pi^+}, x)$ . By symmetry

$$P_{\pi}(r, R, \theta_{\pi^+}, x) = P_{\pi}(r, R \sin \theta_{\pi^+}) P_{\pi}(x, R \cos \theta_{\pi^+}),$$

where

$$P_{\pi}(r, R \sin \theta_{\pi^+})$$

$$= \begin{cases} 1 & \text{if } R \sin \theta_{\pi^+} \leq R_0 - r, \\ \frac{1}{\pi} \cos^{-1} \left( \frac{R^2 \sin^2 \theta_{\pi^+} + r^2 - R_0^2}{2rR \sin \theta_{\pi^+}} \right) & \text{if } R \sin \theta_{\pi^+} > R_0 - r, \end{cases}$$

and

$$P_{\pi}(r, R \cos \theta_{\pi^+})$$

$$= \begin{cases} 1 & \text{for } -l/2 - R \cos \theta_{\pi^+} \leq x \leq l/2 \\ 0 & \text{outside} \end{cases} \quad \cos \theta_{\pi^+} < 0,$$

$$= \begin{cases} 1 & \text{for } -l/2 \leq x \leq l/2 - R \cos \theta_{\pi^+} \\ 0 & \text{outside} \end{cases} \quad \cos \theta_{\pi^+} > 0.$$

The probability that the decay muon which has a range  $a = 9$  cm in  $H_2$  remains within the target can be written in the form

$$P_{\mu}(r, R, \theta_{\pi^+}, x, a) = P_{\mu}(a, r, R \sin \theta_{\pi^+}) P_{\mu}(a, x, R \cos \theta_{\pi^+}),$$

where

$$P_{\mu}(a, r, R \sin \theta_{\pi^+})$$

$$= \frac{1}{4\pi} \int P_{\pi}(r + a \sin \theta', R \sin \theta_{\pi^+}) \sin \theta' d\theta' d\varphi',$$

and

$$P_{\mu}(a, x, R \cos \theta_{\pi^+})$$

$$= \frac{1}{4\pi} \int P_{\pi}(x + a \cos \theta', R \cos \theta_{\pi^+}) \sin \theta' d\theta' d\varphi'.$$

One then has

$$F_+(R, \theta_{\pi^+}) = \frac{1}{V} \int P_{\mu}(r, \theta_{\pi^+}, R, x, a) \frac{\Omega(x', y', z')}{4\pi} dx' dy' dz',$$

where  $x', y', z'$  are the coordinates of the end point of the  $\mu^+$ . Finally using the kinematics for process (3) one can transform  $F_+(R, \theta_{\pi^+})$  into  $F_+(E_{\gamma}, \theta_{\pi^+}^*)$ .

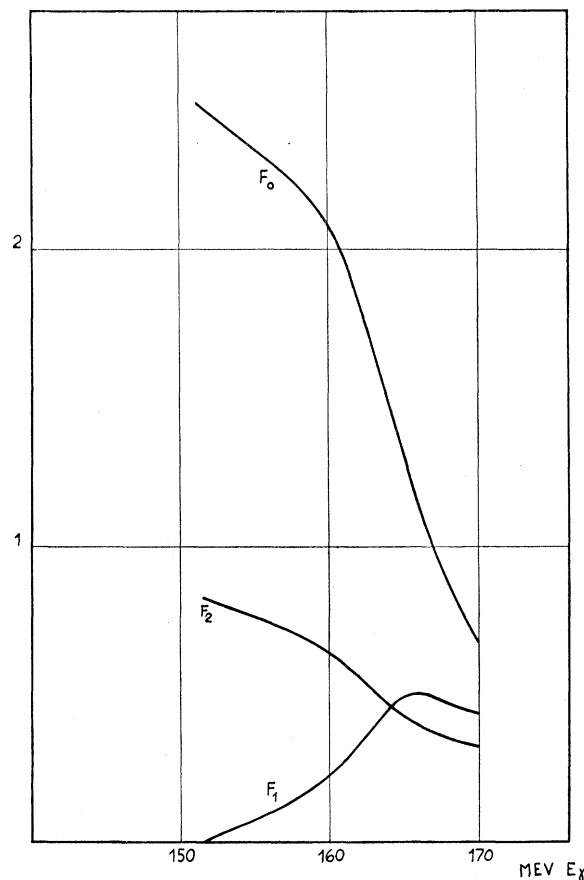
In Fig. 11 are plotted three functions proportional to  $F_0, F_1, F_2$  computed by using the values of  $a_0, a_1$ , and  $a_2$  published in reference 3. In the calculation, the 3-mil Cu longitudinal walls of the target have been transformed in an equivalent liquid  $H_2$  thickness.

#### 4. ANALYSIS OF THE DATA

##### (a) Absolute energy calibration of the x-ray beam

If one assumes that there exists an energy shift between the nominal maximum energy  $E_{\gamma}$  of the bremsstrahlung spectrum and its absolute value  $E_{\gamma}^{(a)}$ , one can write

$$Z(E_{\gamma}) = \frac{Y_+(E_{\gamma})}{K'_{H_2}(E_{\gamma})} = \alpha F(E_{\gamma}^{(a)}),$$

FIG. 11. The functions  $F_0, F_1, F_2$  as a function of  $E_{\gamma}$ .

where  $Z(E_\gamma)$  is the observed yield (corrected for the monitor) at the nominal maximum x-ray energy  $E_\gamma$  and  $F(E_\gamma^{(a)})$  is the theoretical yield function calculated on the basis of the previous considerations at an absolute x-ray energy  $E_\gamma^{(a)} = E_\gamma + \epsilon$ ;  $\alpha$  represents a normalization constant. In order to evaluate the function  $F$  an hypothesis is needed at least on the energy dependence, of the three coefficients  $a_0, a_1, a_2$  of the angular distribution of process (3). Because of the predominance, in our energy region, of the large  $S$ -wave term, the energy dependence of  $F$  is not strongly affected by the choice of  $a_1$  and  $a_2$ . So the values of  $a_1$  and  $a_2$  reported in (3) have been chosen. For  $a_0$  we chose two cases:

Case I.

$$a_0 = \text{const. according to (3).}$$

Case II.

$$a_0 = \frac{\text{const}}{k\omega} \left\{ 1 - \frac{v^2}{2k^2} - \frac{g_p + g_n}{M} \omega \left( 1 - \frac{v^2}{2} \right) \right\},$$

according to the dispersion relations calculation as quoted by Cini *et al.*<sup>12</sup> In order to determine the absolute energy calibration of the x-ray beam, one has to evaluate the energy shift  $\epsilon$  necessary to match the experimental values of  $Z(E_\gamma)$  with the evaluated  $F(E_\gamma^{(a)})$ . If one presumes to know the last function, then by assuming the energy shift to be small, one can write

$$Z(E_\gamma) = \alpha F(E_\gamma) + \alpha \epsilon (\partial F / \partial E_\gamma)_{E_\gamma},$$

and by a least squares fit, deduce the value of  $\epsilon$ . This procedure is justified, from one side by having an estimate of the shift by a calibration based on a betatron magnetic field calibration, from another side by a check *a posteriori*.

By following such a procedure it was found that

$$\epsilon = (-1.38 \pm 0.17) \text{ Mev for case 1,}$$

$$\epsilon = (-1.63 \pm 0.17) \text{ Mev for case 2.}$$

These two values are equal within the errors. Thus by this comparison, one cannot decide between the two cases. The decision would have been possible if the constant  $\alpha$  was known, i.e., if we could reliably evaluate the absolute efficiency of our detection system.

#### (b) $\pi^0$ 's from He

Up to energies of 160 Mev, the photoproduction of neutral pions from He is elastic. Because the total angular momentum of the  $\alpha$  particle is zero, the matrix element for the process will not be dependent on the Pauli spin operator and its general form will be

$$T = (\mathbf{k} \times \mathbf{e}) \cdot \mathbf{q} f(k, \cos \theta_{\pi^0}^*),$$

where  $f$  is an unknown function of  $k$  and  $\theta_{\pi^0}^*$ . The

angular distribution will be, in general, proportional to

$$\sin^2 \theta_{\pi^0}^* |f(k, \cos \theta_{\pi^0}^*)|^2,$$

corresponding to the fact that the  $\pi^0$  must be in a  $p$  state so that the cross section must be proportional to  $q^3 \sin^2 \theta_{\pi^0}^*$ . To make explicit the function  $f(k, \cos \theta_{\pi^0}^*)$ , use can be made of the impulse approximation in order to use the production amplitude on single nucleons. Under this hypothesis,

$$T = \langle f | \sum_{j=1}^4 T_j | i \rangle,$$

where  $|i\rangle$  and  $|f\rangle$  are the initial and final wave functions of the  $\alpha$  particle. In general,

$$T_j = e^{i(\mathbf{k}-\mathbf{q}) \cdot \mathbf{r}_j} [(\mathbf{k} \cdot \boldsymbol{\sigma}_j + L) + (\mathbf{M} \cdot \boldsymbol{\sigma}_j + N) \tau_j^3]$$

while for the specific case of the process under consideration because the  $\alpha$  particle has  $T=0, J=0$

$$T = 4LF_r(q^2),$$

where  $F(q^2)$  is the He charge form factor ( $q$  is the 3-dimensional momentum transfer to the  $\alpha$  particle).

The dispersion relations calculation gives

$$L = (\mathbf{k} \times \mathbf{e}) \cdot \mathbf{q} \{ \lambda h^{(+)} + (4/9) i e^{i\alpha_{33}} \sin \alpha_{33} F_M \}.$$

So that the differential cross section, by assuming  $f^2 = 0.88$  turns out as

$$d\sigma/d\Omega^* = 45.6 \times 10^{-30} (a_{11} + 2a_{13} + a_{31} + 4a_{33})^2 k q^3 \sin^2 \theta_{\pi^0}^* F_r^2(q^2),$$

where  $a_{2T, 2J}$  represent the scattering lengths for the corresponding phase shifts.

#### $\pi^0$ Mass from He

To obtain the mass of the  $\pi^0$  from He a theoretical yield curve was calculated. The threshold of the experimental yield curve was obtained from the energy dependence of the theoretical yield curve. Since  $F_r^2(q^2)$  is a slow function of  $E_{\gamma \text{ max}}$  in our energy region, the cross section was written as

$$d\sigma/d\Omega^* \simeq A k q^3 \sin^2 \theta_{\pi^0}^* \text{ with } A \text{ constant.}$$

A yield curve was obtained by multiplying  $d\sigma/d\Omega^*$  by  $F_{\text{He}}(E_\gamma')$  and integrating over the bremsstrahlung spectrum. If this curve is plotted on log-log paper it is found to be a straight line from threshold to 150 Mev.

From the slope, it is determined that

$$Y_{\text{He}} \propto (E_\gamma - E_{\gamma \text{ th}})^{2.22}.$$

After subtracting the background, the  $1/2.22$  power of the experimental points was plotted against  $E_\gamma$ . These experimental points also lie in a straight line for energies under 150 Mev. The extrapolation of the experimental points to zero yield gives the threshold value of the reaction. Using the  $\pi^+$  experiment as an energy calibration of the betatron gives as the value of the mass of the

<sup>12</sup> M. Cini, R. Gatto, E. L. Goldwasser, and M. Rudermann, *Nuovo cimento* **10**, 243 (1958).



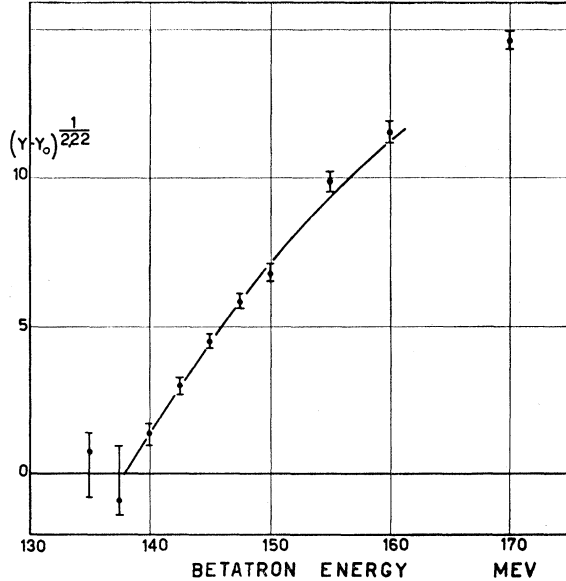


FIG. 12. Threshold determination for process  $\gamma + \text{He}^4 \rightarrow \pi^0 + \text{He}^4$ .

$\pi^0$  meson from He  $136 \pm 1$  Mev. Figure 12 shows the  $1/2.22$  power of the experimental yield points and also of the theoretical yield curve normalized to fit the experimental points under 150 Mev. This curve also seems to fit the points at higher energies. The mass value obtained is in agreement with the value obtained in the zero kinetic energy  $\pi^-$  charge exchange process. This result adds some evidence against the Baldin's proposal of the existence of the  $\pi_0^0$  meson.<sup>13</sup> Such a proposal was advanced two years ago in order to remove an inconsistency which seemed to exist in the comparison, by means of the Panofsky ratio, between the experimental data on low-energy charged meson photoproduction and the measured  $s$ -wave scattering phase shifts. According to Baldin, the known neutral meson with mass  $m_0 = 135$  Mev was a pion ( $\pi_0^0$ ) with total isotopic spin  $T=0$ . Furthermore, he proposed that the ordinary neutral pion ( $\pi^0$ ) with  $T=1$  and  $T_3=0$  had a mass close to that of the charged pion, namely,  $m_0' \simeq m_+ = 139.7$  Mev.

#### Small $p$ -Wave Scattering Lengths

The normalization of the theoretical yield curve for He with the experimental results gives for the constant  $A$

$$A = (5.2 \pm 0.02) \times 10^{-30} \text{ cm}^2.$$

For the low-energy points from which the constant  $A$  was determined  $\bar{F}_r^2(q^2) \simeq 0.6$ . Taking  $a_{33} = 0.217$ , which is consistent with  $f^2 = 0.088$  and in good agreement with recent experimental results,<sup>14</sup> one gets

$$a_{11} + 2a_{13} + a_{31} = -0.433.$$

<sup>13</sup> N. Booth, O. Chamberlain, and E. Rogers, Bull. Am. Phys. Soc. 4, 446 (1959).

<sup>14</sup> S. W. Barnes, B. Rose, G. Giacomelli, J. Ring, K. Miyake, and K. Kinsey, Phys. Rev. 117, 226 (1960); J. E. Fisher and E. W. Jenkins, Phys. Rev. 116, 749 (1959).

According to the effective range formulas for the small  $p$ -wave phase shifts given by C.G.L.N. this sum turns out equal to  $-0.309$ . So the experimental result seems to suggest at least qualitatively, the validity of the scattering lengths predicted by the C.G.L.N. effective-range formulas. This conclusion seems quite surprising because by using the C.G.L.N. effective-range formulas to evaluate the small  $p$ -wave phase shifts in the high-energy region where they are experimentally known (although with large errors), the predictions are in complete disagreement with experiment, except for the  $a_{31}$  phase shift. For example the  $a_{11}$  phase shift is predicted with an opposite sign. If use is made of the high-energy experimental points to extrapolate to low energy by means of effective-range formulas one gets

$$a_{11} + 2a_{13} + a_{31} \simeq 0.010.$$

Recently, however, Bowcock, Cottingham, and Lurie<sup>15</sup> have calculated the effect of the inclusion of a  $\pi-\pi$  interaction term in the calculation of the scattering lengths. The added term due to the  $\pi-\pi$  interaction does not change substantially the scattering lengths predicted by the effective range formulas (it turns out  $a_{11} + 2a_{13} + a_{31} \simeq -0.264$ ) but its energy dependence seems to show that it might change substantially the energy dependence of the predicted phase shifts so as to bring good agreement with the experimental data.

#### (c) $\pi^0$ 's from Hydrogen

According to the dispersion relation calculation of Chew *et al.*, the c.m. differential cross section for the photoproduction of neutral pions from  $\text{H}_2$  can be expressed as

$$d\sigma/d\Omega^* = A + B \cos^2 \theta^*_{\pi^0} + C \cos^2 \theta^*_{\pi^0}.$$

The coefficients of the angular distribution can be expressed as

$$A = \frac{e^2 f^2 q}{m_0^2 k} (|E_1|^2 + A_{0p}),$$

$$B = \frac{e^2 f^2 q}{m_0^2 k} [2kq \text{Re}(E_1^* K)],$$

$$C = \frac{e^2 f^2 q}{m_0^2 k} (|K|^2 k^2 q^2 - A_{0p}),$$

where  $q$  is the c.m. pion momentum,  $k$  the c.m. photon energy (both in units  $\mu$ ), and  $\theta^*$  is the c.m. pion angle from the x-ray direction.  $E_1$  is the  $s$ -wave amplitude,  $K$  the spin-flip  $p$ -wave amplitude, and  $A_{0p}$  is the contribution to the cross section of the no-spin-flip  $p$  wave. In the square of the complete amplitude given by Chew *et al.* also appears a  $D \cos^2 \theta^*$  term, which at the energies of this experiment is always negligible. Besides this

<sup>15</sup> J. Bowcock, W. N. Cottingham, and D. Lurie, preprint (to be published).

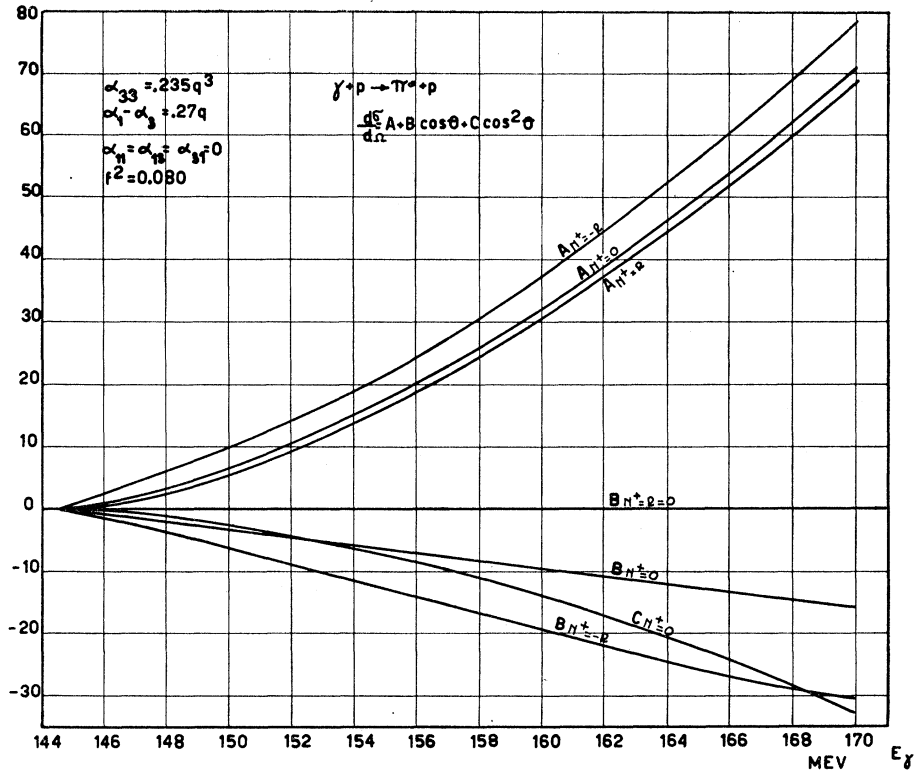


FIG. 13. Coefficients of the angular distribution for the process  $\gamma + p \rightarrow \pi^0 + p$  as they result from the C.G.L.N. calculation with the specified assumptions.

term there is also an addition to the term given for  $B$ . At the energies of this experiment this term is also negligible. The transition amplitudes are given by Chew *et al.* explicitly in terms of the scattering phase shifts, and of the pion nucleon coupling constant  $f$ . The structure of the  $s$ -wave amplitude is particularly interesting:

$$E_1 = \frac{2}{3}i(\alpha_1 - \alpha_3)F_s + \omega\alpha(N^+ - R).$$

The first term corresponds to the production of a  $\pi^+$  with a subsequent charge exchange scattering on the parent nucleon. In this term  $F_s$  is a function of  $q$  which describes the large  $s$  wave  $\pi^+$  transition amplitude,  $\alpha_1$  and  $\alpha_3$  are the  $s$ -wave scattering phase shifts corresponding to  $T = \frac{1}{2}$  and  $T = \frac{3}{2}$ . In the second term, the  $-R\omega\alpha$  part is a recoil term which is also responsible for making the threshold value of the  $\pi^-/\pi^+$  ratio larger than one.  $\alpha = [1 + (\omega/M)]^{-1}$  is a kinematical factor introduced in each recoil term to properly take into account the phase space factor.  $R = (g_p + g_n)/2M$  is explicitly evaluated by Chew *et al.* in terms of the physical proton and neutron magnetic moments  $g_p$  and  $g_n$ . These enter by evaluation of the  $1/M$  corrections to the first approximation static solution of the dispersion integrals.  $N^+$  is a real electric dipole amplitude given by the authors in the form of a dispersion integral whose evaluation seems to be quite difficult. So  $N^+$  was considered to be unknown and Chew *et al.* suggest it is constant and no larger than 0.2 in absolute value. In the comparison

made below,  $N^+$  was assumed energy independent and its absolute value was assigned to give the best agreement with the experimental data. The comparison with the experimental results will be made by evaluating the theoretical yield curve obtained by multiplying the theoretical values of  $A$ ,  $B$ , and  $C$  by their respective efficiency functions and then integrating over the pion angles and bremsstrahlung spectrum.

This direction has been chosen, since the experiment was done only at one angle, and without some argument as to the energy dependences of  $A$ ,  $B$ ,  $C$  it is impossible to extract the values of the coefficients. Various theoretical assumptions to calculate  $A(E_\gamma)$ ,  $B(E_\gamma)$ , and  $C(E_\gamma)$  have been made, and theoretical yield curves have been evaluated to compare with the experimental data. Since in the first comparison there was no agreement, we began to search for ways to fit the data. Thus, we list various attempts to achieve agreement, stating some sort of reason for the attempt and calculating the consequent angular distribution and yield curve. It is singularly unfortunate that the H<sub>2</sub> experiment was performed at only one angle, as the theoretical yield curve at our angles is not very sensitive to the various assumptions made. Besides our interest in the possible validity of some of the various assumptions, there was always concern that none of the assumptions was such as to produce complete agreement with the experiment. Various other possible effects are discussed at the end, but not calculated.

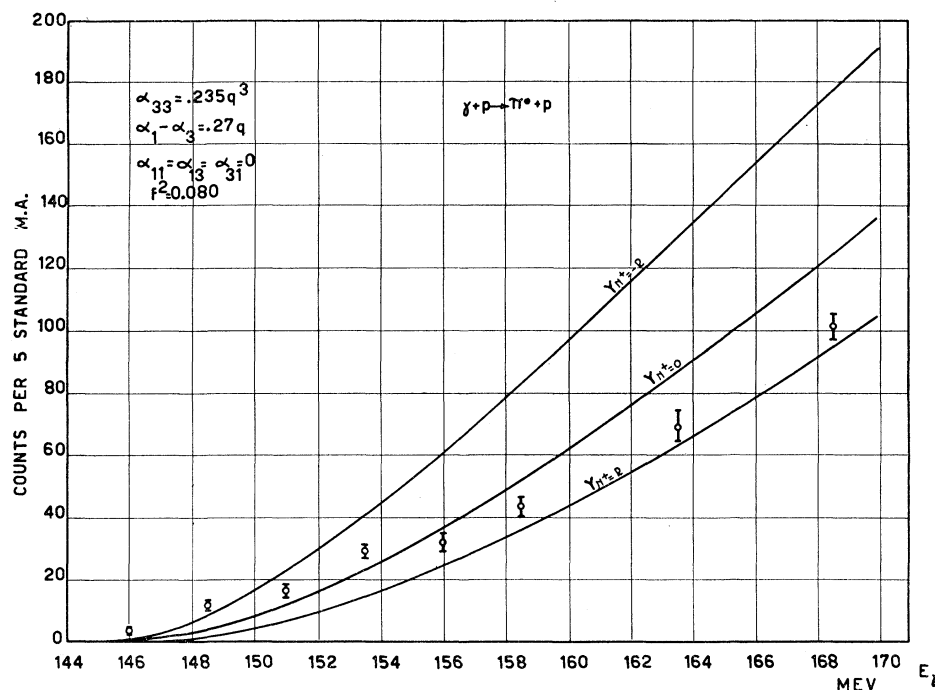


FIG. 14. Comparison of the hydrogen experimental yield with the yield curve evaluated by using the  $A$ ,  $B$ , and  $C$  of Fig. 12 and the efficiency functions of Fig. 8.

In the evaluation of the theoretical yield curves, we always assumed  $\alpha_1 - \alpha_3 = 0.27q$ .<sup>16</sup> In the first calculation performed, we chose  $f^2 = 0.080$ ,  $\alpha_{33} = 0.235q^3$  according to the Orear fit,  $N^+ = 0$  and  $\alpha_{11} = \alpha_{13} = \alpha_{31} = 0$ . In the graphs which follow the experimental points have been shifted according to the value of  $\epsilon$  deduced from the fitting of the  $\pi^+$  yield curve. The comparison shows that at all energies there are deviations of the calculated yield from the experimental one. At energies above 155 Mev, agreement can be achieved if we choose  $N^+ \simeq R = (g_p + g_n)/2M$ . With this  $N^+$ , the experimental yield at low energies is higher than the theoretical one. However if  $N^+ = R$ , it must be clearly stated that the asymmetry part of the angular distribution  $B$ , goes almost to zero, which is in contradiction with experiments which have measured the angular distribution.<sup>6,10</sup>

If  $N^+ = -R$  the values of  $B$  is about double that of the case of  $N^+ = 0$ . Furthermore the theoretical yield curve while in a bit better agreement with the very low-energy points is badly in disagreement with the higher energy measurements. We thus feel that a positive value for  $N^+$  is most probable. Figures 13 and 14 show the angular distributions and the yield curves for  $N^+ = -R, 0, +R$ .

Since none of these yield curves fit the data, the next thing that was tried was to determine the effect of the small  $p$ -wave phase shifts. The value of these phase shifts was calculated in two different ways. The first was to extrapolate the experimental values<sup>17</sup> of these phase shifts around  $q=2$  to low energies by means of an effective range type formula. This gave values near

threshold of  $\alpha_{11} = +0.055q^3$ ,  $\alpha_{31} = -0.45q^3$ ,  $\alpha_{13} = 0$ . The effect of introducing these phase shifts into the formulas hardly changed  $A$ ,  $B$ , and  $C$ . Thus also the change in the theoretical yield curve was very small. Figure 15 shows this yield curve for  $N^{(+)} = 0$ .

The second method of evaluating the  $p$ -wave phase shifts was to use, coherently with the He results, the effective-range formulas of Chew *et al.* In this case we used a somewhat different value of  $\alpha_{33}$  and  $f^2$ . From the  $\alpha_{33}$  effective-range plot including new data,<sup>14</sup> we determined  $f^2 = 0.088$  and  $\omega_2 = 2.17$ . At low energies this combination leads to  $\alpha_{33} = 0.217q^3$ . Using the relativistic corrections to the effective range formulas,  $\alpha_{11}$ ,  $\alpha_{13}$ , and  $\alpha_{31}$  were evaluated as functions of  $q$ . In the range of  $0 \leq q \leq 0.55$ , these phase shifts cannot be expressed in the manner  $\alpha_{TJ} = a_{TJ}q^3$  with  $a_{TJ}$  constant. Instead the actual calculated value of the phase shift was used. The striking part of these calculated small  $p$ -wave phase shifts is the large negative value predicted for  $\alpha_{11}$ . Very close to threshold, the value of  $a_{11}$  determined by dividing  $\alpha_{11}$  by  $q^3$  is  $-0.167$  which is 77% of  $a_{33}$ . However, in the extrapolation to higher energies, the values of  $\alpha_{11}$  are in disagreement, both in sign and in magnitude, with the experimental scattering data. Introducing these phase shifts into the formulas radically changed the angular distribution, Fig. 16, making  $C$  positive instead of negative. The effect on the theoretical yield curve at the angle of the experiment was reasonably small and again there was agreement with the four higher energy points for  $N^+ = R$  and disagreement with the four lower energy points, Fig. 17.

The agreement in shape of the He experiment with

<sup>16</sup> J. Orear, Nuovo cimento 4, 856 (1956).

<sup>17</sup> B. Pontecorvo, Ninth International Conference on High-Energy Physics, Kier, 1959 (unpublished).

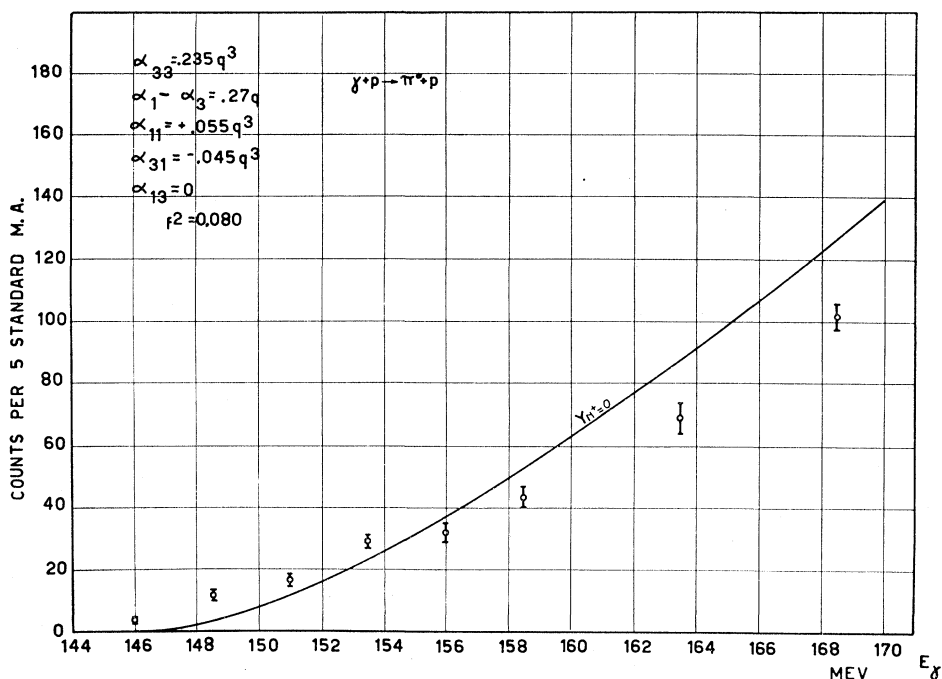


FIG. 15. Comparison of the hydrogen experimental yield with the curve evaluated by extrapolating to threshold the experimental values of the small  $p$ -wave phase shifts.

the theoretical yield curve predicted for it, leads us to conclusion that the difficulty in  $H_2$  was either in the  $S$ -wave charge exchange scattering term or in the recoil terms, both of which are lacking in  $\pi^0$ 's from  $He$  but present in  $\pi^0$ 's from  $H_2$ .

In conclusion below 155 Mev there is no agreement with the C.G.L.N. formulas when  $N^+$  is assumed constant. This could be ascribed to the fact that the theoretical calculation does not take into account  $\pi^+ - \pi^0$  mass difference while the energy interval where the

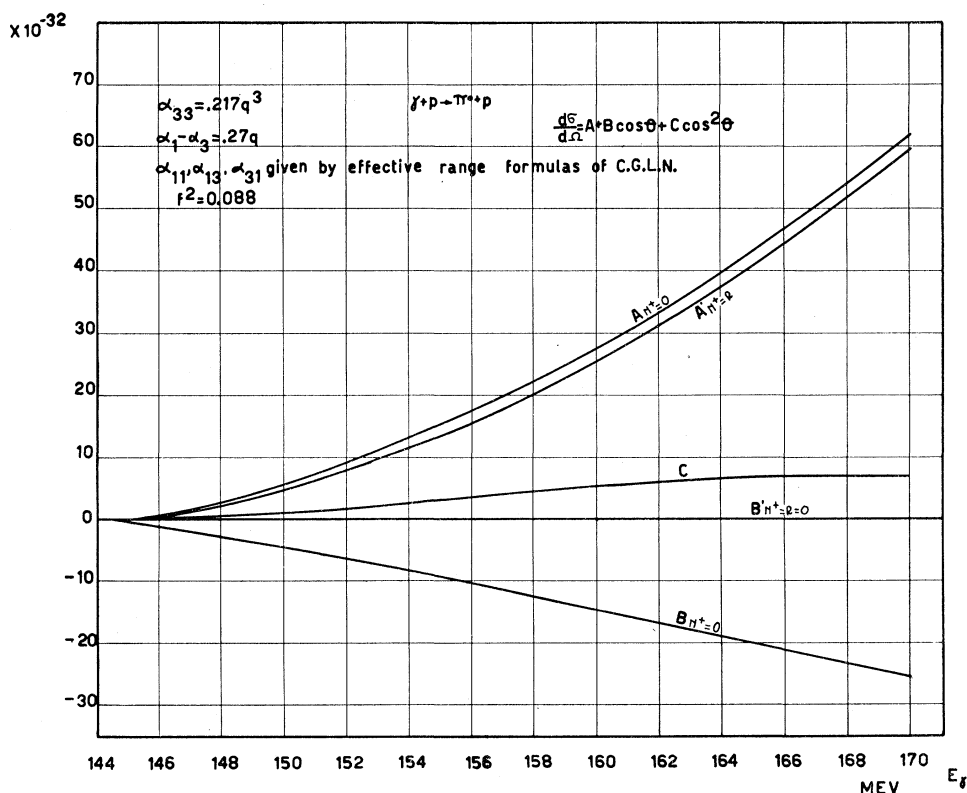


FIG. 16. Coefficients of the angular distribution of the process  $\gamma + p \rightarrow \pi^0 + p$  obtained by the C.G.L.N. evaluation and by using for the small  $p$ -wave phase shifts the values obtained by using the effective-range formulas.

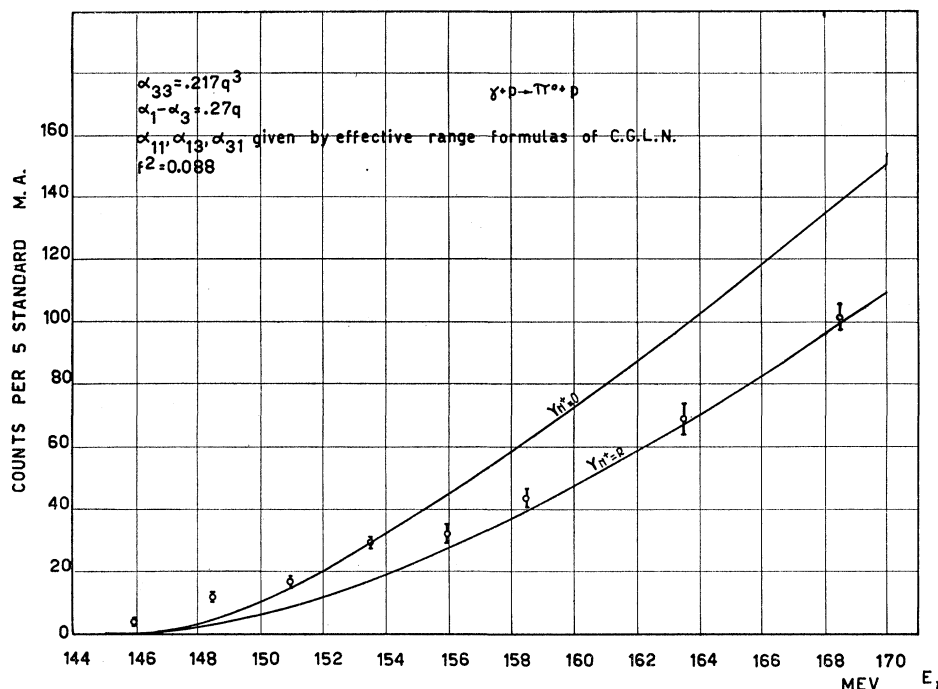


FIG. 17. Comparison between the experimental yield and the yield curve evaluated with the same assumptions of Fig. 15.

disagreement exists is just the one between the thresholds of charged and neutral processes. For instance, below the  $\pi^+$  threshold which is at  $E_\gamma = 151.2$  Mev, the  $S$ -wave term corresponding to the production of a  $\pi^+$  meson with a subsequent charge exchange scattering, must be equal to zero. Unfortunately this correction (which is the only one we have been able to think of) would make the disagreement between the theoretical yield curve and experimental one even worse, since the correction removes a contribution to the yield curve.

Assuming that the deviation was due to a term which had to be added to the  $S$  wave, we took the difference between the experimental and theoretical curve for  $N^+ = R$ , and by using the  $S$ -wave efficiency function  $F_A$ , we determined that the amplitude of the needed term was probably of magnitude about equal to  $0.2 \simeq 3R$  near the  $\pi^0$  threshold and fell rapidly to zero by the  $\pi^+$  threshold. This could be ascribed to  $N^+$  possibly being energy dependent near threshold and the function needed is the difference between  $N^+$  and  $R$ .

Another way of getting agreement is to add to the amplitude  $\mathcal{F}^{(0)}$  a term which decreases with energy.

The effect of the pion-pion interaction would appear in the recoil amplitude. Cini and Munczek have evaluated such a contribution by assuming the  $\pi-\pi$  system in a resonant state with  $T=1$ ,  $J=1$ . This contribution contains a parameter  $\lambda_0$  which characterizes the strength of the  $\pi-\pi$  interaction. The term is similar to a direct interaction term and like the direct interaction term contains all multipoles. It is interesting to note that since this term appears in  $\mathcal{F}^{(0)}$ , it has a large influence on the  $\pi^-/\pi^+$  ratio. At the angle at which our

$\pi^0$  experiment was performed, the yield curve is not very sensitive to this term. In any case, the term has the wrong energy dependence to cause the observed bump in the experimental yield curve.

No conclusion can be drawn now about the contribution to the photomesonic processes of the  $\pi-\pi$  interaction term. This is so because there seems to be a certain number of unknown parameters in the low-energy region. One of these is  $N^+$  which though we have not evaluated, we believe can be from the expression given by C.G.L. N. at least by a numerical integration. A second parameter is  $\lambda_0$  which may influence the angular distribution of  $\pi^0$  from  $H_2$  also at low energies mainly in the term  $B$  but also in all terms. Other parameters might be the constants to be introduced to take into account the high-energy contribution to the dispersive integrals. These constants can be only determined by the experiment. Not completely known is the combination of small  $p$  wave phase shifts which appear in  $h^{(++)}$ . This combination influences the angular distribution of  $\pi^0$ 's from  $H_2$  mainly in the term  $C$  at low energies. However, the total cross section of elastic  $\pi^0$  from He is very sensitive to this combination so to allow its experimental determination. This is true within the limits in which the use of the impulse approximation for process (2) is valid. Finally the effect of the  $\pi^+-\pi^0$  mass difference must be taken into account.

Since there are so many parameters, it is very difficult to extract very much information from the present experiment. The only conclusion is that the experimental data are not fitted by the C.G.L.N. calculation as it

stands. A new experiment which includes an angular distribution using the two counters geometry would probably supply some of the answers to the unknown parameters especially if the value of  $N^+$  is evaluated as a function of energy below and above the  $\pi^+$  threshold.

### CONCLUSIONS

(1) From the comparison between the values for the threshold for the photoproduction of positive pions from  $H_2$  and neutral pions from He, the mass of the neutral pion from He, comes out to be  $136.1 \pm 1$  Mev if the mass of the positive pion is taken as 139.7 Mev.

(2) The experimental results on the photoproduction of neutral pions from  $H_2$  are generally in accord with the C.G.L.N. dispersion relations calculation above  $E_\gamma = 155$  Mev especially for  $N^+$  positive and of magnitude about equal to that of the  $S$  wave recoil term  $(g_p + g_n)/M$ .

(3) Below  $E_\gamma = 155$  Mev there seems to be some disagreement between the experimental results and our use of the C.G.L.N. formulas. Such disagreement might

be due to any one or combinations of effects such as an energy-dependent  $N^+$  near threshold, the  $\pi-\pi$  interaction, or the  $\pi^+-\pi^0$  mass difference.

(4) Though the present  $H_2$  experiment is not very sensitive to the values of the small  $p$ -wave phase shifts, the angular distribution is affected greatly by their choice, especially in the term  $C$ . The total cross section of elastic  $\pi^0$ 's from He using an impulse approximation calculation is very sensitive to the values of these phase shifts. From the He results we obtain  $a_{11} + 2a_{13} + a_{31} = -0.433$  with a rather small statistical error but with an unknown systematic error. Such a value is in the direction of the predictions given by the C.G.L.N. effective-range formulas.

### ACKNOWLEDGMENTS

We wish to thank Dr. W. John for his great help during the experiment, Professor A. O. Hanson for his advice and Professor M. Cini and Dr. H. Munczek for many useful discussions of the theoretical problems.